

# Analytical model for electron field emission from capped carbon nanotubes

V. Filip

*University of Bucharest, Faculty of Physics, P.O. Box MG-11, Bucharest-Magurele 76900, Romania*

D. Nicolaescu<sup>a)</sup>

*Nanoelectronics Research Institute, AIST, Umezono 1-1-1, Tsukuba, Ibaraki 305-8568, Japan*

M. Tanemura and F. Okuyama

*Department of Environmental Technology, Nagoya Institute of Technology, Gokiso-cho, Showa-ku, Nagoya 466-8555, Japan*

(Received 6 October 2003; accepted 29 March 2004; published 1 June 2004)

This article presents a model of electron field emission from quantum states arising from the tight confinement of quasi-free electrons on a nanotube hemispherical cap. The model outlines the possibility of inhomogeneous electron field emission for very thin carbon nanotubes at high emission levels and the appearance of peculiar ring-shaped field emission images. The conclusions qualitatively agree with existing experimental evidence, therefore supporting the hypothesis that part of the electrons on the cap of the emitter may behave as quasi-free in a high emission level/high-temperature regime. © 2004 American Vacuum Society. [DOI: 10.1116/1.1752902]

## I. INTRODUCTION

Due to their interesting field emission properties, carbon nanotubes (CNTs) are currently under active investigation. While significant progress has been achieved in this field, the details of the electron emission properties of such cathodes are still not clearly understood. Both experimental<sup>1-8</sup> and theoretical simulation efforts<sup>9,10</sup> have disclosed many peculiarities of CNT field electron emission that cannot be explained by the corresponding field enhancement only.<sup>9</sup> One of the main conclusions drawn from these works is that the electronic states localized near or at the apex of the CNT greatly influence the current emission profile. At low or moderate extraction fields, the electron emission from CNTs seems to proceed mainly through such localized states on the tip,<sup>3</sup> where the anode extraction voltage produces the largest local field (as long as the axis of the CNT is perpendicular to the anode plane). The field emission images usually show one central spot or small groups of spots that appear to be symmetrically arranged close to the center. When increasing the anode voltage, the thermal effect brought in by the large emission currents tends to stimulate the emission from cap sites closer to the CNT body. This frequently complicates the field emission images giving rise to emission rings or auras surrounding the central emission spots.<sup>1-8</sup> It was found that the ring-shaped emission images closely precede structural changes of the CNT tip.<sup>1,2</sup> On the other hand, analogous rings were observed from conventional field emitters too, when operated at high fields/high emission currents.<sup>11,12</sup> One may thus be led to link such phenomena to field emission from some nonlocal states that may arise under severe external perturbations, which may induce a continuum behavior of the electronic system: The electron localization should be relaxed from the tight neighborhood of the atomic sites to the

entire CNT cap. A continuous model seems therefore to be more suitable for describing such situations. The main purpose of this article is to give a possible explanation for the apparition of inhomogeneous field emission images in terms of a tunneling theory from nonlocalized electrons on the CNT cap. Assuming that for high emission currents/high local temperatures, part of the electrons of the CNT cap behave as quasi-free, this article proposes a model of spatial confinement quantization of their states and of tunneling field emission from these states into the vacuum. The (already tested) simple two-dimensional free electron gas picture<sup>13</sup> was used for this purpose and was applied to a hemispherical configuration of a CNT cap. The states arising on the hemispherical sheet determine an axial probability distribution for the presence of an electron on the cap of the CNT: On average, the probability of finding an electron in a small axial interval increases when moving toward the cylindrical body. On the other hand, it is well known that, as long as the axis of the emitter is perpendicular to the anode plane, the extraction field shows a variation with the polar angle of the emitting site for any field emitter,<sup>14</sup> with a maximum at the tip and a decrease toward the body of the emitter. These two opposite trends lead to an enhancement of the lateral field emission for high extraction voltages. A field emission image projected onto the flat plane of the anode may thus become inhomogeneous in intensity showing darker regions separating external circular auras from the brighter central spots. This result may explain, at least partially, the observed shifting from spotlike to ring-shaped emission images from single CNTs<sup>1-8</sup> when the extraction voltages attain high enough values.

The influence of CNT heating on the apparition of inhomogeneous field emission images is also investigated through the related increase of the surface density of the quasi-free electrons.

<sup>a)</sup>Author to whom correspondence should be addressed; electronic mail: n-dan@aist.go.jp

## II. PHYSICAL MODEL

In the one electron approximation of our continuous model, the Schrödinger equation should be solved for the two-dimensional sheet of the hemispherical cap of the CNT. The azimuth angle  $\varphi$  and the axial coordinate  $z$  (with the origin at the center of the hemisphere and the positive sense toward the vacuum) will be considered as position parameters. Denoting the CNT radius by  $r_0$ , one may also find it useful to use the relative axial position  $\zeta = z/r_0$  instead of  $z$ . The equation for the wave function  $\Psi(\zeta, \varphi)$  of the quasi-free electron on the hemisphere may be obtained in non-Cartesian coordinates by using well known procedures.<sup>15,16</sup>

$$-\frac{\hbar}{2m_0 r_0^2} \left[ \frac{\partial}{\partial \zeta} \left( (1 - \zeta^2) \frac{\partial \Psi}{\partial \zeta} \right) + \frac{1}{1 - \zeta^2} \frac{\partial^2 \Psi}{\partial \varphi^2} \right] = (E + W_0) \Psi, \quad (1)$$

where  $m_0$  is the free electron mass,  $E$  is the total energy of the electron, and  $-W_0$  is its potential energy (assumed to be position independent). The origin for the energy scale will be taken at the chemical potential of the electronic system. The one-electron wave functions also have to satisfy the following normalization condition:

$$\int_0^1 \int_0^{2\pi} |\Psi_l^m(\zeta, \varphi)|^2 d\varphi d\zeta = 1. \quad (2)$$

The normalized solutions of Eq. (1) that remain finite at the CNT tip ( $\zeta=1$ ) and nonvanishing at the body–cap interface ( $\zeta=0$ ) can be readily written as<sup>16</sup>

$$\Psi_l^m(\zeta, \varphi) = \sqrt{\frac{2l+1}{2\pi} \frac{(l-m)!}{(l+m)!}} P_l^m(\zeta) e^{im\varphi}, \quad (3)$$

where  $l=0,1,2,\dots, m=-l, -l+1, \dots, l, l+m=\text{even number}$ , and  $P_l^m$  is the corresponding associated Legendre function. The corresponding eigenenergies are therefore given simply by

$$E_l = -W_0 + \frac{\hbar^2}{2m_0 r_0^2} l(l+1). \quad (4)$$

Each energy level  $E_l$  is thus  $(2l+1)$  times degenerate with respect to the quantum number of the axial angular momentum,  $m$ .

The normalization condition of Eq. (2) suggests that a probability density for the electron axial localization can be defined, which will be used in our subsequent field emission analysis:

$$\Pi_l^m(\zeta) = \int_0^{2\pi} |\Psi_l^m(\zeta, \varphi)|^2 d\varphi = (2l+1) \frac{(l-m)!}{(l+m)!} (P_l^m(\zeta))^2. \quad (5)$$

Thus, according to Eq. (5),  $\Pi_l^m(\zeta) d\zeta$  gives the probability of finding a  $(l, m)$ -state electron in a circular strip area of extent  $dz = r_0 d\zeta$ , around the axial position  $z = r_0 \zeta$ , as shown in Fig. 1(a).

The assumed quasi-free one-electron waves on the CNT cap are supposed to mix so that the electronic states described by Eq. (3) are to be occupied according to some

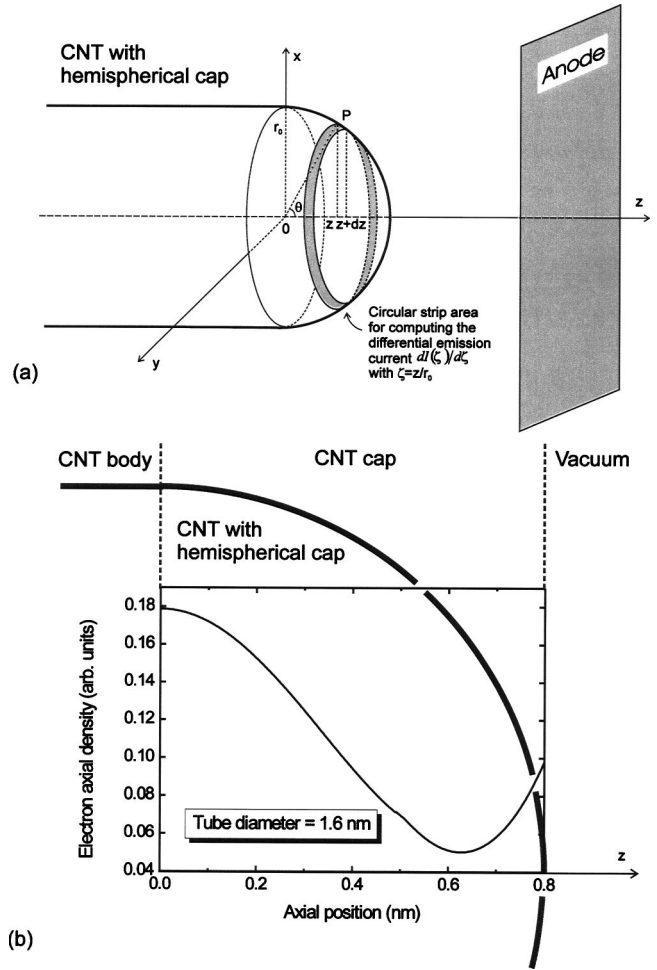


FIG. 1. (a) Field emission configuration considered for the present theoretical analysis. For each infinitesimal circular strip area on the CNT cap, a specific amount of available electrons and a local extraction field is considered. (b) Detail of the configuration depicted in (a) showing the axial variation of the electron population on the cap of a CNT with the diameter  $2r_0 = 1.6$  nm.

statistical distribution. For convenience, this will be approximated by a Fermi–Dirac function, corrected for the spin and  $m$  degeneracy:

$$f(E_l) = 2(2l+1) \left[ 1 + \exp\left(\frac{E_l}{k_B T}\right) \right]^{-1}. \quad (6)$$

As the origin of the energy scale is at the chemical potential, the parameter  $W_0$  appearing in Eqs. (1) and (4) is strongly related to the quasi-free electron surface density on the CNT cap,  $n_s^{\text{free}}$ , which is given by the following equation:

$$n_s^{\text{free}} = \frac{1}{2\pi r_0^2} \sum_{l=0}^{\infty} f(E_l). \quad (7)$$

It may be found useful to express this electron density in relative values with respect to its maximum, which results by counting both  $\pi$ -electrons normally assigned to each graphene hexagon:<sup>17</sup>  $n_s^{\text{max}} = 4/a^2 \sqrt{3}$ , where  $a$  is the lattice constant of graphene ( $a = 2.46 \text{ \AA}$ ).<sup>17</sup>

It is interesting to observe that, by combining the Fermi factor of Eq. (6) with the axial probability density defined by Eq. (5), one may construct the actual electron density along the axis of the hemispherical cap of the CNT. The quantity  $[1 + \exp(E_l/k_B T)]^{-1} \Pi_l^m(\zeta) d\zeta$  may be interpreted as the probability of finding an electron, having the quantum state  $(l, m)$ , on the CNT cap in the strip defined by  $\zeta$  and  $\zeta + d\zeta$ . Therefore, the probability of finding any electron in that strip amounts to the sum taken over all the quantum states and the total axial electron density is written as

$$\frac{dn_s^{\text{free}}}{d\zeta} = \frac{1}{2\pi r_0^2} \sum_{l=0}^{\infty} f(E_l) \sum_{\substack{m=-l \\ (l+m=\text{even})}}^l \Pi_l^m(\zeta). \quad (8)$$

In Fig. 1(b), as an example, this quantity is plotted as a function of the axial position, for a tube having the diameter  $2r_0 = 1.6$  nm.

The electronic states described by Eq. (3) carry no axial current. Therefore, the tunneling of an electron between such states and the states in the vacuum should be described in the framework of decay phenomena by using the semiclassical concept of attempt-to-escape rates:<sup>18,19</sup>

$$\nu_l^m = \frac{v_l^m}{2t}, \quad (9)$$

where  $t$  is the so-called localization parameter and  $v_l^m$  is a characteristic velocity of the state  $(l, m)$ .<sup>19</sup> As localization parameter, the radius  $r_0$  of the hemispherical cap seems to be the most convenient choice. In order to get a convenient value for the characteristic velocity, one has to address the way an electron enters the cap in the state  $(l, m)$  coming from the body of the tube. The energy of a quasi-free electron on the cylindrical sheet of the body of the CNT can be obtained in a similar way to Eq. (4):<sup>13</sup>

$$E_m(k) = -W_0 + \frac{\hbar^2 k^2}{2m_0} + \frac{\hbar^2}{2m_0 r_0^2} m^2, \quad (10)$$

where  $k$  is the quasi-continuous axial wave vector of the electron and  $m$  is again the quantum number of the axial angular momentum. The electronic potential energy on the body of the tube will be considered to take the same value as on the cap. The axial symmetry of both the cylinder and its cap allows us to assume that the transition of the electron from the CNT body to the cap preserves its axial angular momentum. By further assuming that the aforementioned transition is elastic [therefore by equating the energies of Eqs. (4) and (10)], one may readily obtain a selective expression for the wave vector of an electron that enters the cap of the CNT:

$$k = \frac{1}{r_0} \sqrt{l(l+1) - m^2}, \quad (11)$$

where the quantum number  $m$  has the same limitations as in Eq. (4). Hence, the characteristic velocity may be defined as the axial group velocity of the incoming electron:

$$v_l^m = \frac{\hbar k}{m_0} = \frac{\hbar}{m_0 r_0} \sqrt{l(l+1) - m^2} \quad (12)$$

and the attempt-to-escape frequency becomes

$$\nu_l^m = \frac{\hbar}{2m_0 r_0^2} \sqrt{l(l+1) - m^2}. \quad (13)$$

The tunneling probability from the states described by Eq. (3) into the vacuum states may be computed in the same semi-classical framework, according to well-known results.<sup>20</sup> Assuming a simple triangular potential energy barrier for the electron at the vacuum interface, the tunneling probability gets a simple form depending on the local extraction field in vacuum.<sup>13</sup> The extraction field on a spherical cathode facing a plane anode was found to depend on the particular site on the sphere where the emission takes place.<sup>14</sup> As the assumed perpendicularity of the axis of the cathode on the anode plane allows the electric field to be azimuthally symmetric [Fig. 1(a)], its strength on the CNT cap will depend on the axial position only  $[F(\zeta)]$  and is expected to increase steadily when  $\zeta$  varies from 0 to 1. Accordingly, the tunneling probability will bear the same  $\zeta$  dependence through the local extraction field:

$$D_l(\zeta) = \exp\left[-\frac{4}{3} \frac{\sqrt{2m_0} (\chi - E_l)^{3/2}}{\hbar eF(\zeta)}\right], \quad (14)$$

where  $\chi$  is the work function of the CNT cap. A typical value of 4.7 eV was used for  $\chi$  throughout this article.

Our main concern in the present study is to outline the inhomogeneity of the emission current emerging from the CNT cap due to both the extraction field variation and quantum localization of the available electrons. For this purpose, we were led to construct a suitable quantitative measure for this effect. First, one may assert that, according to the usual definitions,<sup>18,19</sup> the product  $ef(E_l)\nu_l^m D_l(\zeta)$  should represent the tunneling current emerging from the electronic state  $(l, m)$  at the axial site  $\zeta$ . But this definition is incomplete without the inclusion of a proper weight describing the probability that the electron is actually around this site. Therefore, the aforementioned current should be properly expressed by  $ef(E_l)D_l(\zeta)\nu_l^m \Pi_l^m(\zeta) d\zeta$ . Thus, the axial distribution of the total emission current (i.e., the emission current from the CNT cap circular strip between the normalized coordinates  $\zeta$  and  $\zeta + d\zeta$ ) is given by

$$\frac{dI}{d\zeta}(\zeta) = e \sum_{l=0}^{\infty} f(E_l) D_l(\zeta) \sum_{\substack{m=-l \\ (l+m=\text{even})}}^l \nu_l^m \Pi_l^m(\zeta). \quad (15)$$

Using the explicit forms of  $\Pi_l^m(\zeta)$  and  $\nu_l^m$  given by the Eqs. (5) and (13), respectively, and the properties of the associated Legendre functions,<sup>21</sup> the axial distribution of the total current (or, with a shorter name, the differential emission current) from the CNT hemispherical cap becomes

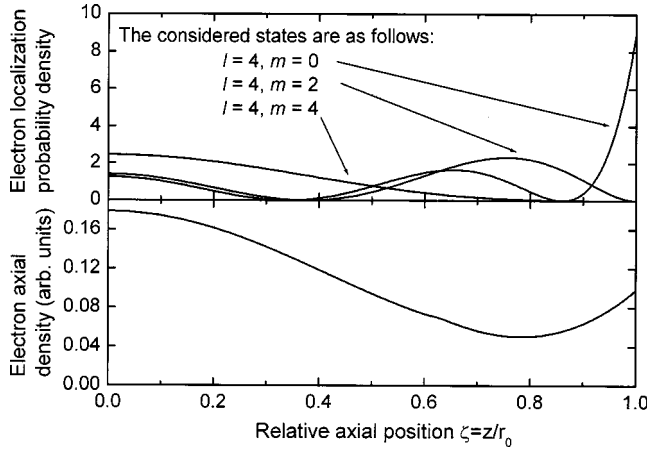


FIG. 2. (a) Axial distribution of the electron localization probability on a CNT hemispherical cap for several possible electronic states. (b) Axial distribution of the total electron density on the CNT hemispherical cap. The relative axial position  $\zeta = z/r_0$  is used for both diagrams.

$$\frac{dI}{d\zeta}(\zeta) = \frac{e\hbar}{2m_0 r_0^2} \sum_{l=0}^{\infty} (2l+1) f(E_l) D_l(\zeta) \times \sum_{j=0}^l \sqrt{l+4jl-4j^2} \frac{(l-|2j-l|)!}{(l+|2j-l|)!} (P_l^{2j-l}(\zeta))^2. \quad (16)$$

While still complicated, Eq. (16) can be used for further analysis through numerical computation.

### III. RESULTS AND DISCUSSIONS

The inhomogeneity of the electron field emission over a CNT cap may have two distinct sources: The spread in the quantum/statistical localization of the electrons on the sheet of the cap and the site variation of the local extraction field. We examine in Fig. 2 the first source of emission inhomogeneity. In Fig. 2(a), the electron localization probability density  $\Pi_l^m(\zeta)$  computed through Eq. (5) is represented for several states. As one can see, the electrons carrying high axial angular momentum (high absolute values of the quantum number  $m$ ) tend to concentrate toward the CNT body. In Fig. 2(b) [also plotted in the inset of Fig. 1(b)], account is taken of the statistical occupation probabilities by computing the axial electron density [Eq. (8)]. The expected relatively high values at the tip region are separated by a certain gap from the more consistent densities found toward the body/cap interface.

The second main source of emission inhomogeneity is the site variation of the local extraction field. When the tube is perpendicular to the anode plane, we expect a maximum value of the electric field at the tip and a monotonic decrease toward the CNT body. This trend is quite opposite to that of the electron density, which was shown to increase toward the “lateral” area, i.e., toward the cap/body junction. The real nonhomogeneous distribution of the local emission current should thus be the result of the competition of these two factors. The stronger the lateral extraction field, the more

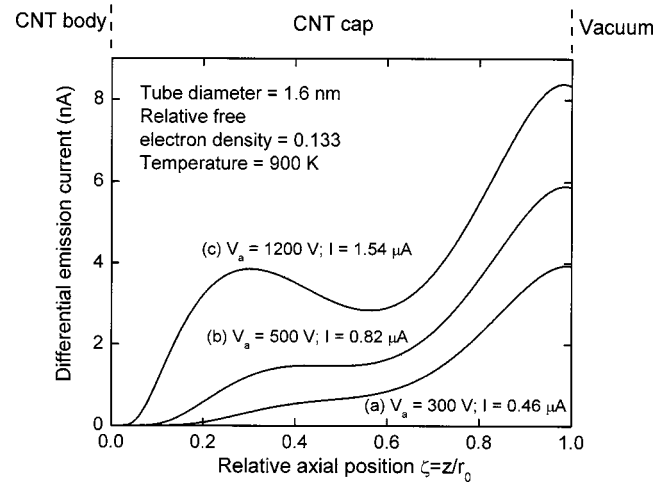


FIG. 3. Axial emission current distributions  $dI(\zeta)/d(\zeta)$  over the closure of a capped CNT for several extraction voltages. The total emission currents  $I$  for each case are also indicated.

highlighted the axial quantum/statistical distribution of electrons. Unfortunately, it is a quite difficult task to construct a specific form of the local extraction field intensity  $F(\zeta)$ . Despite existing elaborate related results,<sup>22,23</sup> no simple analytical dependence of the extraction field on the position of a particular site of a conductive field emission tip is available. In the simple floating sphere model,<sup>23</sup> it is known that the extraction field in the tip area is proportional to the cosine of the local polar angle.<sup>14</sup> For the analysis below, we speculatively extend this dependence over all of the hemisphere of the CNT cap:

$$F(\zeta) = F_0 \cos \theta = F_0 \frac{z}{r_0} = F_0 \zeta, \quad (17)$$

where  $\theta$  is the polar angle as shown in Fig. 1(a). It is clear that the real extraction field is not vanishing at the cap/body interface, as appears in Eq. (17). Also, this choice is less likely to highlight the emission inhomogeneity effect. Nevertheless, obtaining inhomogeneous electron field emission even in such an unfavorable situation would be a significant confidence enhancement that the effect will appear more clearly in real cases. As for the field strength on the tip,  $F_0$ , it is known to be fairly independent on the distance to the anode. In a simplified model, it can be estimated by<sup>13,24</sup>

$$F_0 = \frac{V_a}{s r_0}, \quad (18)$$

where  $V_a$  is the anode potential. The value of the self-screening factor  $s$  is usually taken as 5.<sup>24</sup> More accurate values can be set by comparison with some numerical computations, which show lower figures.<sup>13</sup> However, for demonstrability reasons, we prefer to use the less favorable value of 5. The results obtained by choosing the extraction field in the form given by Eqs. (17) and (18) are illustrated in Fig. 3. The axial distribution of the total emission current is computed using Eq. (16) for several values of the anode potential. The total emission currents [obtainable through in-

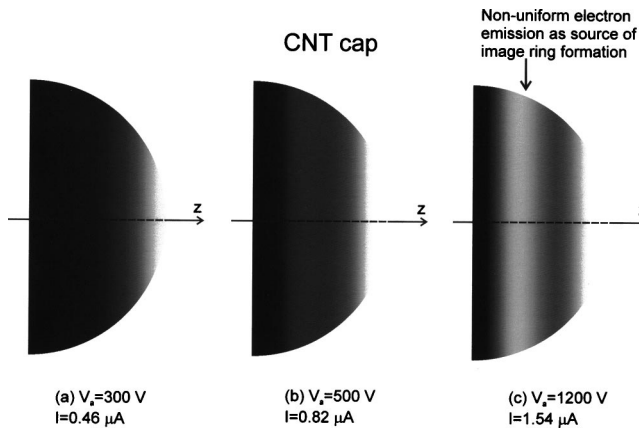


FIG. 4. Axial emission current distributions  $dI(\xi)/d\xi$  over the closure of a capped CNT for several extraction voltage represented as grayscale images. The data used are the same as in Fig. 3, with “white” color attributed to the maximum value of the current density. The images outline the non-uniform electron emission pattern from circular strips [as shown in Fig. 1(a)] on the CNT hemispherical cap as source of anode image ring formation.

tegration of the current axial distribution of Eq. (16)] are also indicated for each curve. It can be seen that the axial distribution of the emission is inhomogeneous even for relatively low anode voltages. Higher voltages produce a still larger effect: The two “brighter” areas become clearly separated by an emission gap.

Figure 4 contains essentially the same information as Fig. 3, but in a more “visual” form: The field emission level is represented here by the brightness of various areas appearing on a profile of the cap of the CNTs. At high voltages, the lateral areas with high electron emission levels become visible as strips on the surface of the cap. In an imaging experiment, this would correspond to two brighter areas: a central one surrounded by a blurred ring of less emissivity (an aura). Such field emission images from individual capped CNTs are indeed reported in literature.<sup>1-3</sup>

At this point, it may be speculated that the ring formation in real cases at high voltage/high emission currents from CNTs could also be due to the contribution of the electrons emitted from the body of the CNTs. Indeed, under high emission current regimes, the self-heating of the CNT may enhance the electron emission even from the body of the tube and the corresponding electron trajectories may be compressed into a ringlike structure. Not ruling out this possibility, we note however that the imperfect perpendicularity of the CNT on the anode plane (expected in real cases) would produce much more deformed (elongated) rings, with much more blurred external parts, than usually observed.<sup>1-3</sup>

For a given value of the parameter  $W_0$ , the diameter of the tube controls the quasi-free electron confinement on the CNT cap. Inhomogeneous electron field emission is to be expected only from very sharp (few nanometers wide) cathodes. Larger cap diameters will allow states with higher  $l$  values to be occupied [see Eqs. (4) and (6)] and will increase the number of significant terms in Eqs. (8) and (16). This will tend to wash out the spatial dependence of the electron

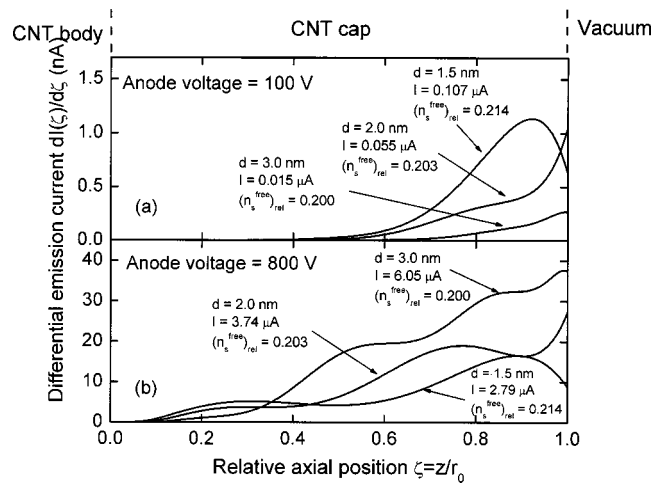


FIG. 5. Axial emission current distributions  $dI(\xi)/d\xi$  over the closure of a capped CNT for several tube diameters  $d = 2r_0$  in both low (a) and high (b) extraction voltage regimes. The total emission currents  $I$  for each case are also indicated.

density or of the current axial distribution. Such a behavior is illustrated in Figs. 5(a) and 5(b). It can be seen that even at relatively low voltages [Fig. 5(a)], very thin tube caps allow for strongly inhomogeneous axial current distribution. As the tube diameter increases, the distribution becomes flatter and contains no special feature. At very high voltages [Fig. 5(b)], the situation is quite similar, but the flattening of the current distribution for larger tubes is less effective. Strong fields may extract electrons even from very lateral sites and can still produce some “waving” of the axial current distribution (multiple ring formation at high extraction voltages have also been reported).<sup>1</sup> Larger tube caps may even accommodate so many electrons that, at high voltages, higher currents may be pulled out from them as compared to the thinner ones, despite the difference in local field enhancement [Fig. 5(b)]. One should be however cautious in practically interpreting such a result since possible field enhancement at localized

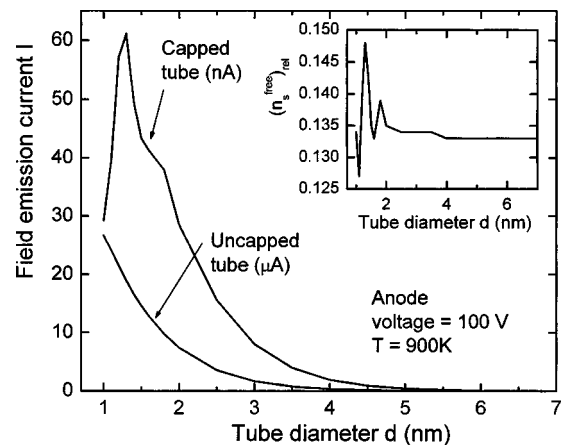


FIG. 6. Dependence of the field emission current  $I$  from a capped CNT, generated by the quasi-free electrons, on the tube diameter  $d$ . The corresponding dependence for opened CNTs is presented for comparison. The inset shows the corresponding diameter dependence of the quasi-free electron density on the CNT cap.

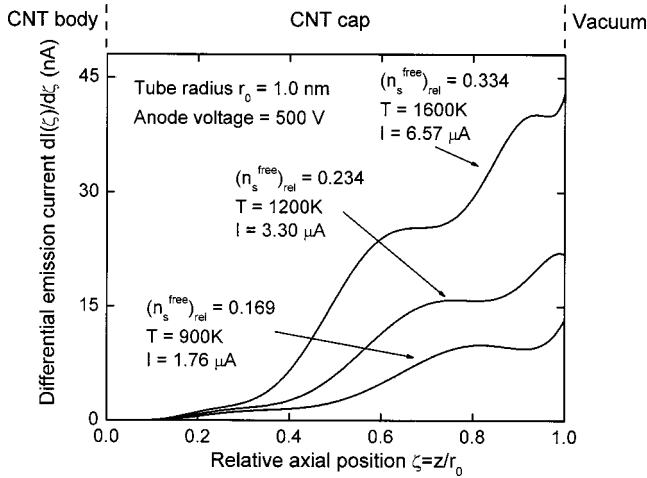


Fig. 7. Axial emission current distributions  $dI(\xi)/d\xi$  over the closure of a capped CNT for several quasi-free electron densities.

states on the cap of the CNT<sup>9</sup> may completely mask the effect of emission current enhancement with increasing CNT diameters.

The contribution of the quasi-free electron states localized on the CNT cap to the field emission is also apparent from Fig. 6, where the emitted current is plotted against the tube diameter. For comparison, the same diagram for an opened CNT, as obtained in Ref. 13, is presented. One may first remark the three orders of magnitude difference between the two sets of current values. No edge-induced field enhancement was considered for an uncapped CNT, so this large difference between the emission currents is to be associated only with very different density of states/attempt-to-escape rates values for the two considered configurations. These results agree with some field emission experiments,<sup>4</sup> where opened CNTs were found to be much more intense electron sources as compared to closed ones. The features appearing in the low-diameter range of the capped CNT curve of Fig. 6 can be explained by the corresponding variation of the electron surface density (see the inset of Fig. 6, where the relative density  $n_s^{\text{free}}/n_s^{\text{max}}$  is plotted against the tube diameter).

The variation of the quasi-free electron surface density may also have an important influence on the axial distribution of the emission current. As can be seen in Fig. 7, the increase of the quasi-free electron population (resulting from both high emission levels and local heating) leads to enhanced emission from the lateral parts of the cap. The increase of quasi-free electron density associated with the local temperature or emission currents increase (local temperatures as high as 2000 K can be attained)<sup>25</sup> may, therefore, render the special features of field emission images to become brighter, sharper, and more complicated (i.e., multiple rings). This behavior seems to be confirmed in experiments with CNT emitters operated at high temperatures/high anode voltages.<sup>1</sup>

#### IV. CONCLUSIONS

By assuming that a certain part of the electrons of the cap structure of a CNT behave as quasi-free, it is concluded that

the tight confinement on the two-dimensional CNT cap induces discrete energy levels from which electron field emission may proceed. The computed axial distribution of the quasi-free electron contribution to the field emitted current reveals the possibility, for very high extraction voltages, of ring (aura) formation around the usual field emission images. This conclusion qualitatively agrees with existing experimental evidence, possibly concurring with other causes (which are not considered in the present approach).

#### ACKNOWLEDGMENTS

One of the authors (V.F.) gratefully acknowledges useful discussions with Professor T. Marian from the Theoretical Physics Department of the Faculty of Physics of the University of Bucharest and with Dr. T. Cheche from the Molecular Physics Department of the same Faculty.

- <sup>1</sup>K. A. Dean, P. von Allmen, and B. R. Chalamala, *J. Vac. Sci. Technol. B* **17**, 1959 (1999).
- <sup>2</sup>K. A. Dean and B. R. Chalamala, *J. Vac. Sci. Technol. B* **21**, 868 (2003).
- <sup>3</sup>W. Liu, S. Hou, Z. Zhang, G. Zhang, Z. Gu, J. Luo, X. Zhao, and Z. Xue, *Ultramicroscopy* **94**, 175 (2003).
- <sup>4</sup>Y. Saito, K. Hamaguchi, S. Uemura, K. Uchida, Y. Tasaka, F. Ikazaki, M. Yumura, A. Kasuya, and Y. Nishina, *Appl. Phys. A: Mater. Sci. Process.* **67**, 95 (1998).
- <sup>5</sup>W. Zhu, C. Bower, O. Zhou, G. Kochanski, and S. Jin, *Appl. Phys. Lett.* **75**, 873 (1999).
- <sup>6</sup>J.-M. Bonard, J.-P. Salvetat, T. Stöckli, L. Forró, and A. Châtelain, *Appl. Phys. A: Mater. Sci. Process.* **69**, 245 (1999).
- <sup>7</sup>K. A. Dean and B. R. Chalamala, *Appl. Phys. Lett.* **76**, 375 (2000).
- <sup>8</sup>Y. Saito, K. Hamaguchi, K. Hata, K. Uchida, Y. Tasaka, F. Ikazaki, M. Yumura, S. A. Kasuya, and Y. Nishina, *Nature (London)* **389**, 553 (1997).
- <sup>9</sup>S. Han and J. Ihm, *Phys. Rev. B* **61**, 9986 (2000).
- <sup>10</sup>A. Mayer, N. M. Miskovsky, and P. H. Cutler, *J. Phys.: Condens. Matter* **15**, R177 (1999).
- <sup>11</sup>W. P. Dyke, J. K. Trolan, E. E. Martin, and J. P. Barbour, *Phys. Rev.* **91**, 1043 (1953).
- <sup>12</sup>L. W. Swanson and A. E. Bell, in *Advances in Electronics and Electron Physics*, edited by L. Marton (Academic, New York, 1973), Vol. 32, p. 193.
- <sup>13</sup>V. Filip, D. Nicolaescu, and F. Okuyama, *J. Vac. Sci. Technol. B* **19**, 1016 (2001).
- <sup>14</sup>K. L. Jensen, in *Vacuum Microelectronics*, edited by W. Zhu (Wiley, New York, 2001), Sec. 3, pp. 33–104.
- <sup>15</sup>W. Yougrau and S. Mandelstam, *Variational Principles in Dynamics and Quantum Theory* (Dover, New York, 1979), Sec. 11.
- <sup>16</sup>S. Flügge, *Practical Quantum Mechanics* (Springer, New York, 1974).
- <sup>17</sup>R. Saito, G. Dresselhaus, and M. S. Dresselhaus, *Physical Properties of Carbon Nanotubes* (Imperial College Press, London, U.K., 1998).
- <sup>18</sup>J. W. Gadzuk, *J. Vac. Sci. Technol.* **9**, 591 (1971).
- <sup>19</sup>A. Modinos, *Surf. Sci.* **42**, 205 (1974).
- <sup>20</sup>N. F. Mott and T. N. Sneddon, *Wave Mechanics and its Applications* (Clarendon, Oxford, U.K., 1948).
- <sup>21</sup>M. Abramowitz and I. A. Stegun, *Handbook of Mathematical Functions* (Dover, New York, 1972).
- <sup>22</sup>W. P. Dike, J. K. Trolan, W. W. Dolan, and G. Barnes, *J. Appl. Phys.* **24**, 570 (1953).
- <sup>23</sup>T. Utsumi, *IEEE Trans. Electron Devices* **38**, 2276 (1991).
- <sup>24</sup>R. Gomer, *Field Emission and Field Ionization* (Harvard University Press, Cambridge, MA, 1961).
- <sup>25</sup>S. T. Purcell, P. Vincent, C. Journet, and V. T. Binh, *Phys. Rev. Lett.* **88**, 105502 (2002).